

Silicates—Space and Laboratory

Thomas Henning¹, Harald Mutschke²,
and Cornelia Jäger²

¹Max Planck Institute for Astronomy, Königstuhl 17, D-69117 Heidelberg, Germany
email: henning@mpia.de

²Astrophysical Institute and University Observatory, Schillergässchen 2, D-07745 Jena,
Germany
email: mutschke@astro.uni-jena.de, conny@astro.uni-jena.de

Abstract. In this paper, we will review recent progress made in the understanding of cosmic silicates and the experimental characterization of relevant analogue materials. We will introduce the main structural properties of silicates. Then we will discuss recent infrared observations with a special emphasis on protoplanetary disks and AGNs. In the experimental section we will describe the optical properties of silicate grains. Here we will concentrate on fundamental optical data and the dependence of the optical behavior on particle shape and temperature.

Keywords. astrochemistry — cosmic dust — planetary systems: protoplanetary disks — galaxies: quasars

1. Introduction

Apart from carbonaceous grains, silicates are the major refractory component of interstellar dust. Silicates regulate the thermal structure of regions in space where dust grains dominate the opacity. The various spectral features of silicate particles in the infrared spectral domain are a unique diagnostic tool for the determination of the optical depth of the medium, its temperature, and chemical state as well as for dynamical processes such as turbulent mixing in protoplanetary disks. Silicates provide the surface for chemical reactions and the condensation of volatile components in the cold environments of molecular clouds and the outer regions of protoplanetary disks. Finally, we should stress that silicates are an interesting class of materials with a large variety of physical, chemical, and optical properties.

Due to the large amount of data and the limited space available, we will concentrate on major new developments in the observational characterization of cosmic silicates and the laboratory study of their optical behavior relevant to astronomy. We refer the reader to Henning (2003a) for an extensive review of earlier results and to Colangeli *et al.* (2003) for a detailed discussion of the properties of silicon-based materials. Data from the Infrared Space Observatory ISO and the Spitzer Space Telescope led to the characterization of crystalline silicates in space and, together with data from meteorites and interplanetary dust particles, opened up the new field of astromineralogy (Henning 2003b).

2. Structural Properties of Silicates

The most interesting cosmic silicates belong to the mineral groups of pyroxenes and olivines. The olivine group consists of silicates with the general sum formula $A^{2+}B^{2+}SiO_4$. Here A and B are divalent cations, the most abundant of which in astrophysical environments are Mg and Fe. Mg^{2+} and Fe^{2+} can replace each other in the crystal structure. This means that olivines can be considered as solid solutions of Mg_2SiO_4 and Fe_2SiO_4 ; the

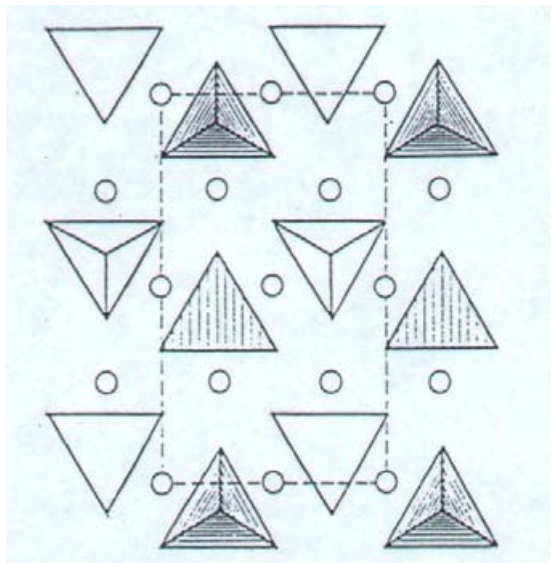


Figure 1. The crystalline structure of olivine. The dashed line marks the border of the elemental cell.

mixture ratio can be expressed by the subscript x in the general formula $\text{Mg}_{2x}\text{Fe}_{2-2x}\text{SiO}_4$ with $1 \leq x \leq 0$. The two end members of the isomorphous crystalline compounds are Mg_2SiO_4 ($x = 1$) and Fe_2SiO_4 ($x = 0$), named forsterite and fayalite, respectively. The mineral “olivine” contains 8 to 20 mass percent FeO. Minerals with higher FeO contents are called hortonolite and ferrohortonolite. The olivines are neso-silicates (island silicates) because they consist of isolated SiO_4 tetrahedra that are linked by divalent cations (see Fig. 1). The metal ions are coordinated by six oxygens. There are two nonequivalent six-coordinate positions in the olivine structure which are both distorted. According to the lattice symmetry, the olivines belong to the rhombic crystal system.

The pyroxenes form a large group of minerals belonging to the inosilicates (chain silicates). The basic structural units of the silicates, the SiO_4 tetrahedra, form $[\text{Si}_2\text{O}_6]_\infty$ chains, i.e. each tetrahedron shares two of its oxygens with the adjacent two tetrahedra. The direction of the chains is the crystallographic c -axis. There are two types of SiO_4 tetrahedral chains with different Si–O distances. Pyroxenes have the symbolic formula $\text{Mg}_x\text{Fe}_{1-x}\text{SiO}_3$. The metal ions, which link the SiO_4 chains, are coordinated by six oxygens (see Fig. 2). There are also two different types of distorted MeO_6 octahedra. Pyroxenes also form solid solution series. The Fe-free and Mg-free end members are enstatite ($x=1$) and ferrosilite ($x=0$), respectively. Enstatite can contain up to 10% of Fe by weight. The minerals with higher Fe^{2+} content are bronzite and hypersthene. In contrast to olivines, pyroxenes can occur in two different main crystallographic systems. The lattice can be of rhombic or monoclinic structure. The rhombic crystal structure is produced by twinning of the unit cell of clinopyroxene by operation of a b -glide parallel to the (100)-plane. This group is called orthopyroxene and represents the most common Mg–Fe pyroxenes. Pyroxenes containing cations with radii considerably larger than that of Mg^{2+} , e.g. Ca^{2+} , belong to the monoclinic system. Under extreme formation conditions, monoclinic Mg–Fe pyroxenes can also be produced, e.g., clinoenstatite. Synthetic Mg pyroxenes produced via melting usually are of this type.

Other groups of crystalline silicates considered as possible dust analogues are hydrous silicates mostly crystallizing in the form of layer silicates (phyllosilicates). In these materials the silicate tetrahedra form a layer with the general formula $(\text{Si}_2\text{O}_5^{2-})_x$ which is combined with an adjacent OH layer. Both belong to an octahedral layer with

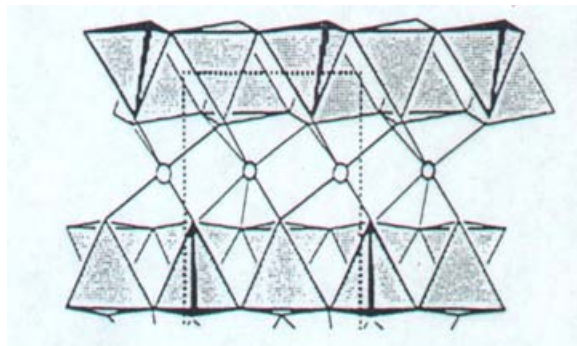


Figure 2. The crystalline chain structure of orthopyroxene.

octahedrally coordinated cations. For example, in the hydrous silicate talc with the chemical formula $\text{Mg}_3(\text{OH})_2[\text{Si}_2\text{O}_5]_2$ brucite ($\text{Mg}(\text{OH})_2$) layers are inserted between the silicate planes. The number of bridging oxygen atoms in these silicates amounts to three. AlO_4 tetrahedra can easily replace the SiO_4 groups and big cations like K^+ , Na^+ , Ca^+ and water molecules can additionally be incorporated in the silicate structure. Besides talc, serpentine ($\text{Mg}_3(\text{OH})_4[\text{Si}_2\text{O}_5]$), chlorite and montmorillonite belong to this phyllosilicate group and represent minerals of certain astrophysical interest. However, the chemical composition of these minerals is rather uncertain and depends on the varying content of water.

Amorphous silicates are built of the same basic structural units, the SiO_4 tetrahedra, but they do not show periodic structures like crystalline silicates. The SiO_4 tetrahedra form a three-dimensional disordered network. The incorporation of metal cations like Fe^{2+} or Mg^{2+} leads to a partial destruction of the oxygen bridges and the formation of non-bridging oxygen (NBO). In the produced hollow space the cations are octahedrally coordinated by such NBOs. However, small cations like Mg^{2+} can act as network formers and can replace the silicon in the SiO_4 groups. The overall number of bridging oxygen atoms depends of course on the general stoichiometry of the silicate. For example in an amorphous MgSiO_3 silicate the average number of bridging oxygen per silicate tetrahedron is 2. However, the resulting amorphous structure can be visualized by mixing of different structural SiO_4 arrangements, like islands, small chains, rings and sheets, on a very small scale (Mysen *et al.* 1982). It is generally known that a phase transition between crystalline and amorphous silicates leads to a dramatic change of their spectral properties from the ultraviolet to the far-infrared region.

Amorphous silicates of pyroxene or olivine composition typically show two broad IR bands at about 10 and 18 μm corresponding to Si–O stretching and bending vibrations. The large width of both bands results from a distribution of bond lengths and angles within the amorphous structure. The 18 μm band is additionally broadened due to the coupling of the Si–O bending to the Me–O stretching vibration in this spectral region (Gervais *et al.* 1987). The position of the Si–O stretching vibration depends on the level of SiO_4 polymerization. For example, the band is shifted from 9 μm for pure SiO_2 to about 10.5 μm for $\text{Mg}_{2.4}\text{SiO}_{4.4}$ (Jäger *et al.* 2003a). Simultaneously, the O–Si–O bending mode is shifted towards shorter wavelengths.

In contrast to amorphous silicates crystalline pyroxenes and olivines produce a wealth of narrow bands from the mid-infrared to the far-infrared range due to metal-oxygen vibrations. Generally, the spectrum can be divided into three main regions. The bands between 1100 and 800 cm^{-1} correspond to different asymmetric and symmetric stretching

vibrations of the SiO_4 tetrahedra. The group of modes in the region between 700 and 470 cm^{-1} can be attributed to bending vibrations of the SiO_4 tetrahedra. The far-infrared bands in the low-frequency region beyond 470 cm^{-1} are caused by translational motions of the metal cations within the oxygen cage and complex translations involving metal and Si atoms. However, more accurate band assignments can be found in the literature (see, e.g., Servoin & Piriou 1973; Hofmeister 1997).

The study of crystalline pyroxenes and olivines with different Mg/Fe ratios has demonstrated that the majority of the IR peaks are shifted to longer wavelengths with growing iron content. The observed shift is caused by an increase of the bond lengths between the metal cations and oxygen when Mg^{2+} is substituted by Fe^{2+} (Cameron & Papike 1980). The wavenumber shift $\Delta\nu$ is closely correlated with the Fe content and promises at least the possibility to derive values of the Mg/Fe ratio of crystalline silicates from the band positions (Jäger *et al.* 1998).

The study of phase conversions from the amorphous into the crystalline state and vice versa are essential for the understanding of astronomical spectra. The conversion from the amorphous into the crystalline state can be caused by annealing at sufficiently high temperatures. Crystallization is a complex process including nucleation and crystal growth. Infrared spectroscopy has been used for monitoring the progress of annealing (see Hallenbeck *et al.* 1998; Fabian *et al.* 2000). The activation energy of crystallization for different amorphous silicate materials has been calculated using the equation $\tau^{-1} = \nu_0 e^{-E_a/kT}$, wherein E_a is the activation energy and ν_0 is a constant proportional to the mean vibrational frequency of the silicate lattice ($\nu_0 = 2.0 \times 10^{13}\text{ s}^{-1}$). The estimation of the required annealing time at a given temperature is then based on the calculated activation energy. Since the crystallization is related to a preliminary diffusion of metal and oxygen atoms, the activation energy is strongly related to the viscosity behavior of the silicate during annealing. Since OH^- ions are able to reduce the viscosity, the annealing temperature as well as the annealing time can be considerably reduced by the presence of OH in the silicate network (Jäger *et al.* 2003a). Apart from annealing of amorphous silicates, crystalline silicates can be formed directly from the gas phase. A gas-phase condensation route for the formation of crystalline silicates in the solar nebula and other protoplanetary disks has been recently discussed by Scott & Krot (2005).

Since the discovery that a significant fraction of stardust silicates leave their stellar environment in crystalline form, the question has arisen of why the interstellar silicate dust component does not show any indications of crystallinity. Amorphization of crystalline silicates due to irradiation by cosmic rays is one possible scenario. Interaction between the solid particles and ions may be expected in an energy range of a few eV up to a few MeV. In the astrophysical context, a series of irradiation experiments on crystalline olivines and pyroxenes were performed (see Bradley 1994; Dukes *et al.* 1999; Demyk *et al.* 2001). An efficient amorphization by light ions like H^+ and He^+ could only be observed for low energies ($\leq 50\text{ keV}$). At very low energies (20 keV H^+ , 4–10 keV He^+) the amorphization process can be accompanied by a selective sputtering of Mg and Si relative to oxygen. Irradiation experiments of submicrometre-sized clinoenstatite (MgSiO_3) particles with 400 keV Ar^+ and 50 keV He^+ ions lead to an amorphization process without a change of the chemical composition but with morphological consequences (Jäger *et al.* 2003c).

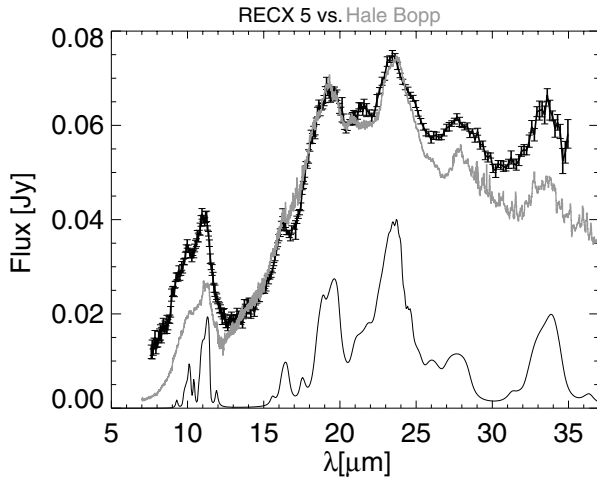


Figure 3. A comparison between the spectra of RECX5 and Hale-Bopp. The lower line is an emission spectrum for a distribution of hollow forsterite spheres (compact equivalent radius of $0.1 \mu\text{m}$) at 200 K. After Bouwman *et al.* (2005).

3. Progress in Space

In this section, we will exclusively concentrate on protoplanetary disks and AGNs and quasars because of the tremendous progress made in the silicate spectroscopy of these objects.

Earlier studies of T Tauri disks showed that the $10 \mu\text{m}$ silicate features occur predominantly in emission (see, e.g., Natta *et al.* 2000). This fact together with models of protoplanetary disks (Menshchikov & Henning 1997; Chiang & Goldreich 1997) clearly suggested the presence of an optically thin surface layer in flaring disks. Here we should note that the feature goes from emission to absorption in the rare cases of protoplanetary disks seen edge-on.

ISO provided the first clear evidence for the presence of crystalline silicates in the spectra of relatively bright Herbig Ae/Be stars (Meeus *et al.* 2001) with HD 100546 (Malfait *et al.* 1998) and HD 163296 (van den Ancker *et al.* 2000) being good examples. Silicates in the diffuse interstellar medium and in molecular clouds are predominantly in the amorphous state. The detection of crystalline silicates in disks implies that they are either produced by annealing of amorphous silicates at higher temperatures in inner regions of disks or form directly from the gas phase. We refer the reader to a discussion of thermal processing of silicate dust in the solar nebula and clues coming from the analysis of primitive chondritic meteorites by Scott & Krot (2005). The amazingly perfect match of the “crystalline” features of HD 100546 with those of comet Hale-Bopp (Crovisier *et al.* 1997) establishes a bridge between circumstellar and cometary material. Most of the features in these two sources can be identified with crystalline forsterite. With Spitzer we are now in the position to measure fainter sources in the mass range of T Tauri stars (see, e.g., Forrest *et al.* 2004). However, we should note that in the $8\text{--}13 \mu\text{m}$ atmospheric window such data are also becoming available from ground-based observatories (see, e.g., Przygodda *et al.* 2003; Kessler-Silacci *et al.* 2005). The disadvantage of these data is obviously the limited wavelength range and the thermal background from the atmosphere. Figure 3 shows a comparison between the Spitzer spectrum of a disk around the M-type star RECX5 (age about 9 Myr) and the ISO spectrum of Hale-Bopp (Bouwman *et al.* 2005), again with a remarkable agreement between these two spectra. Another very interesting Spitzer result is the finding that even spectra of disks around brown dwarfs show evidence for the presence of crystalline silicates (Apai *et al.* 2005). Presently, we are

trying to find out if the fraction of crystalline silicates is a function of stellar or disk mass. There is some indication that disks around more massive stars have a higher fraction of crystalline silicates (van Boekel *et al.* 2005).

Spitzer spectroscopy of older stars with debris disks has usually not led to the detection of features due to silicates. An explanation for this finding may be the fact that the particles have already grown to such sizes that their features are no longer visible. An exception is the remarkable spectrum of the 2 Gyr old star HD 69830, which shows clear evidence for the presence of crystalline silicates (Beichman *et al.* 2005).

Long-baseline interferometry at mid-infrared wavelengths is now opening a new chapter in the study of silicates. For the first time, we are able to determine the radial distribution of silicates in protoplanetary disks. The very first observations of disks around Herbig Ae stars with the MIDI instrument at the Very Large Telescope Interferometer showed that dust in the inner regions of these disks is highly crystallized, more so than any other dust observed in protoplanetary disks so far (van Boekel *et al.* 2004). Figure 4, taken from this paper, clearly shows that the inner-disk spectrum is dominated by crystalline olivine and pyroxene particles. One can exclude a significant contribution from hydrous silicates, clearly pointing to the fact that the dust has not been modified by hydrous alteration. For HD 142527 we even see evidence that the innermost disk regions are dominated by forsterite particles and that the enstatite/forsterite fraction increases with radius. This is in agreement with chemical equilibrium models as well as the radial mixing of material. These models predict that forsterite, present in the innermost disk regions, is converted into enstatite at slightly lower temperatures by a reaction with gas-phase silicon (Gail 2004).

Another important result is the accumulating evidence of the growth of silicate particles in the disk surface layer, from sizes of about $0.1 \mu\text{m}$ to particle sizes of few microns (see, e.g., Bouwman *et al.* 2001; van Boekel *et al.* 2003; van Boekel *et al.* 2005). An interesting recent finding by van Boekel *et al.* (2005) is the observation that all sources with crystalline silicates are dominated by large grains. This issue needs certainly more studies, investigating what happens at longer wavelengths and how much this conclusion is influenced by the increasing contrast between “crystalline” features and the flatter profiles of larger silicate grains.

We will now discuss new observational results concerning silicate features in AGNs and quasars. The unified models for AGNs assume that the central black hole is surrounded by dusty material that absorbs light from the central source. Many models assume the presence of a somewhat clumpy circumnuclear torus. In the unified picture of AGNs the different types of AGNs are produced by a different viewing angle. In the case of AGNs of Type 2, the torus is seen edge-on and the 10 and $18 \mu\text{m}$ silicate features should be seen in absorption. In the case of Type 1 AGNs (face-on view) the features should occur in emission. As discussed before, this behavior of the silicate feature has been found in protoplanetary disks of different orientation. Furthermore, the mid-infrared spectra of many Type 2 AGNs show silicate absorption features. However, Type 1 AGNs have never shown clear evidence for any silicate feature. A variety of models have been developed to explain this behaviour ranging from tori with larger grains, to anisotropic radiation coming from the accretion disk, to clumpy tori. However, recent observations with the IRS spectrometer on board the Spitzer Space Telescope led to the detection of 10 and $18 \mu\text{m}$ emission in a number of radio-quiet and radio-loud quasars (Hao *et al.* 2005; Siebenmorgen *et al.* 2005). Meanwhile, silicate emission features have also been detected in the spectra of AGNs of lower luminosity (Sturm *et al.* 2005). Here, we should note that the inferred dust temperatures are lower than what we would expect for silicates located in the hot torus walls or their surfaces. This may actually indicate that the silicates are

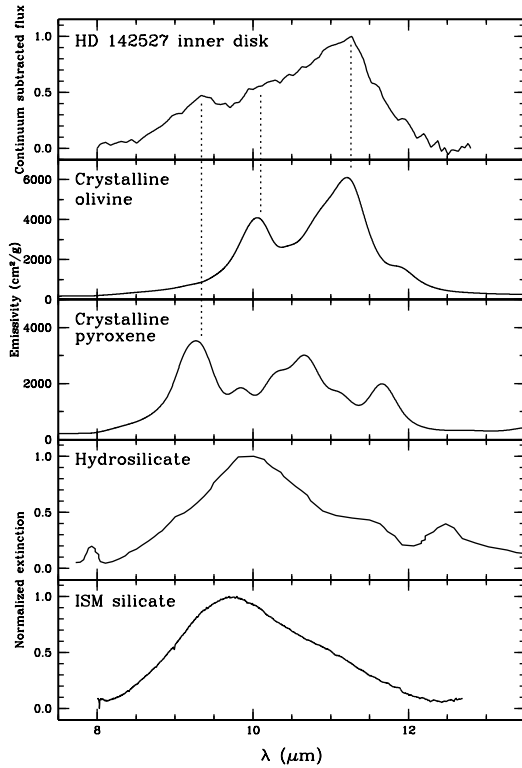


Figure 4. The spectrum of the innermost regions of HD 142527 compared with the laboratory spectra of typical dust species. After van Boekel *et al.* (2004)

not directly associated with the torus, but located in its optically thin environment. In addition, the silicate profiles are different from galactic interstellar medium dust, pointing to the presence of larger grains and differences in the chemical composition.

4. Progress in the Laboratory

Following the recent observational discoveries, especially with ISO, the spectroscopic data of relevant silicates have been considerably refined in collaboration between observers and laboratory astrophysics groups. Especially in the case of crystalline silicates, new optical constants of the most important pyroxene and olivine crystals have been derived (Jäger *et al.* 1998; Fabian *et al.* 2001; Suto *et al.* 2002), and the dependence of the IR band positions on the chemical composition has now been studied in great detail (Chihara *et al.* 2002; Koike *et al.* 2003). For amorphous silicates, the database so far consisting mainly of the optical constants of glasses produced from melts (Dorschner *et al.* 1995; Mutschke *et al.* 1998) and of silicate films (Scott & Duley 1996) has been broadened by new optical constants of sol-gel products with different Mg/Si ratios (Jäger *et al.* 2003a; see Fig. 5). The optical constants of these materials, which often comprise not only the mid- and far-infrared but also the UV and the important near-infrared spectral ranges, are available for observers and theoreticians from WWW databases such as the ones found at <http://www.kyoto-phu.ac.jp/labo/butsuri> and <http://www.astro.uni-jena.de/Laboratory/OCDB> (Henning *et al.* 1999; Jäger *et al.* 2003b). Furthermore, efforts have been undertaken in order to study the dependence of silicate spectral properties on morphological factors, i.e. grain size and shape, as well as on the grain temperature. We will review some of the latest results on these topics in the following discussion.

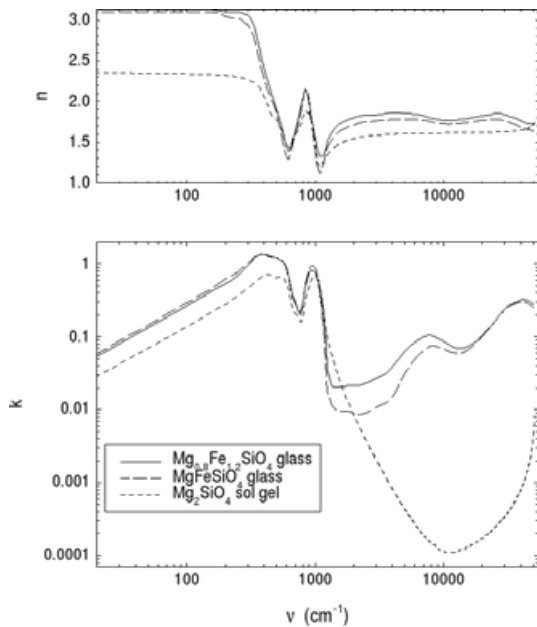


Figure 5. Optical constants of amorphous silicates with olivine stoichiometry: Mg-Fe silicates (glasses) by Dorschner *et al.* (1995), Mg silicate (sol-gel) by Jäger *et al.* (2003).

The influence of the grain morphology (size, shape, agglomeration, porosity) on both the IR band profiles and the far-IR continuum emission or absorption was noted a long time ago. For both cases, theoretical investigations so far dominate over experimental studies, because it is generally very difficult and expensive to control agglomeration, grain shape, and often even grain size in laboratory experiments. Whereas numerical simulations of morphological effects in the far-infrared continuum have led to a good understanding of the effects of porosity, fluffiness, or even metallic inclusions (e.g. Henning & Stognienko 1996), in the mid-infrared bands theoretical approaches often encounter problems with convergence because of the relatively large optical constants. Currently, this seems to be overcome by the development of efficient statistical approaches, which are able to simulate the extinction and emission cross sections of inhomogeneous grains by layered- or hollow-sphere models (Voshchinnikov *et al.* 2005; Min *et al.* 2005). Figure 6 demonstrates how these new theoretical models can be used together with the available optical constants to derive band profiles of non-spherical silicate grains for a mineralogical analysis of the 10 μm band of Herbig Ae/Be stars (from van Boekel *et al.* 2005). Laboratory measurements would be extremely important for the validation of these theoretical results. So far, shape effects on laboratory-measured crystalline silicate bands have been noted in a couple of papers (e.g. Fabian *et al.* 2001; Koike *et al.* 2005), but systematic measurements are still lacking. Recently, first attempts have been made to avoid the influence of embedding media on IR spectroscopy of particulate samples by dispersing particles in air (Tamanai *et al.* 2005), which is a first step to disentangle morphological effects.

The profiles of vibrational bands generally depend on the temperature of emitting or absorbing grains, because of the anharmonicity of the vibrational potentials (Henning & Mutschke 1997). The question of whether this effect can be used as a thermometer has become especially important after the discovery of crystalline silicates in many environments (see, e.g., Bowey *et al.* 2002; Molster *et al.* 2002). Crystalline olivines, e.g., possess promising sharp and isolated far-infrared bands at about 49 μm and 69 μm wavelength, which broaden and shift to larger wavelengths with increasing temperature (Bowey *et al.*

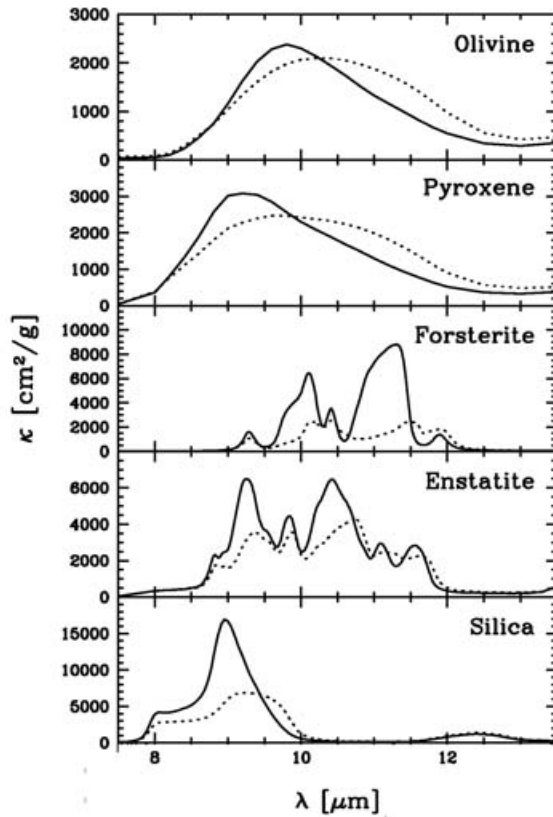


Figure 6. Mass absorption coefficients of amorphous and crystalline silicate grains with volume equivalent radii of $0.1 \mu\text{m}$ (solid lines) and $1.5 \mu\text{m}$ (dotted lines) calculated using the hollow-sphere model (from van Boekel *et al.* 2005).

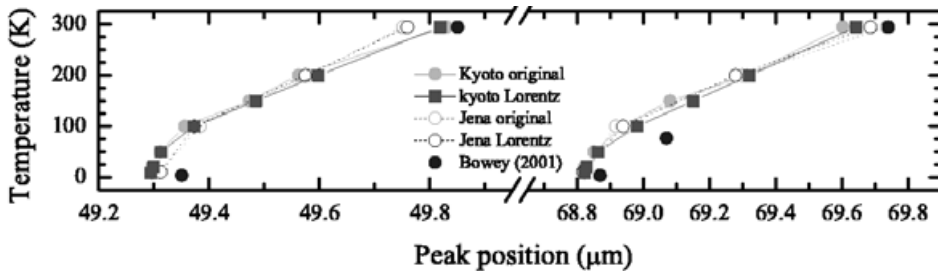


Figure 7. Temperature dependence of the far-infrared peak positions measured in the Kyoto and Jena laboratories on two different synthetic forsterites (Mg_2SiO_4) (from Koike *et al.* 2005). Labels “original” and “Lorentz” refer to the determination of the peak position just by reading by eye and by fitting of a Lorentzian band profile, respectively. Previous data by Bowey *et al.* (2001) are shown for comparison.

2001; Chihara *et al.* 2001). The exact temperature dependence of the peak position of this and other bands has recently been independently measured by two laboratories and has turned out to be nonlinear with stronger changes at higher temperatures (Fig. 7; Koike *et al.* 2005).

The far-infrared continuum absorption of crystalline silicates is known to be strongly temperature-dependent. However, the far-infrared emission of astronomical sources will often be dominated by absorption by amorphous grains, the temperature-dependence of which is less well known. First experimental studies on this subject for astronomically

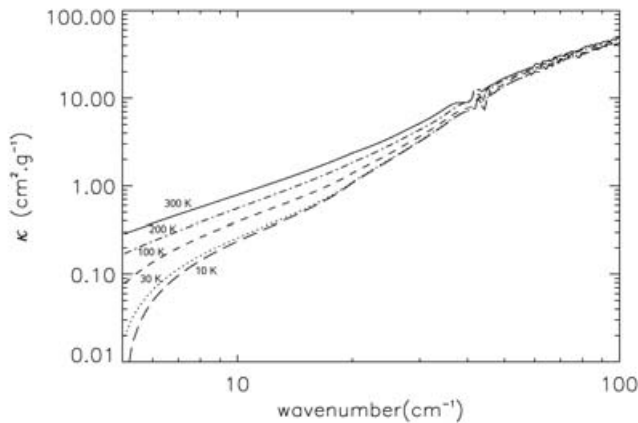


Figure 8. Mass absorption coefficient of MgSiO_3 glass for temperatures between 10 K (long-dashed line) and 300 K (solid line) (from Boudet *et al.* 2005).

relevant amorphous silicates have been carried out by Agladze *et al.* (1996) and Mennella *et al.* (1998), which recently have been extended by Boudet *et al.* (2005). It has been confirmed by these studies that the absorption/emission cross section of amorphous silicates at submillimeter and millimeter wavelengths is significantly lower (up to more than an order of magnitude) at 10 K compared with room temperature (Fig. 8). The spectral power-law index of the opacity's slope at these wavelengths may increase from about unity to values between two and three. This behavior, which is due to transitions in two-level systems probably formed by network-modifier cations, apparently correlates with an observed change of the power-law index in the submillimeter emission of ISM dust at different temperatures (Dupac *et al.* 2003).

Recently, the information about cosmic silicates obtained from infrared spectroscopy has been extended by the analysis of presolar silicate grains in primitive meteorites (Mostefaoui & Hoppe 2004; Nguyen & Zinner 2004), antarctic micrometeorites (Yada *et al.* 2005), and interplanetary dust particles (Messenger *et al.* 2003). These grains are found to be olivines, pyroxenes, and amorphous silicates originating from AGB stars and supernovae, in accordance (apart from the relative abundances) with the spectroscopic information from evolved objects.

5. Summary and Outlook

Over the last several years, we have seen a tremendous progress in our understanding of cosmic silicates, mainly coming from infrared spectroscopy and the chemical and isotopic analysis of primitive meteorites and interplanetary dust. This progress would not have been possible without the efforts of laboratory astrophysics groups, which provided the necessary experimental data for an adequate interpretation of astronomical spectra. We now have available a fundamental database of the optical properties of the most important silicate components. Experiments to clarify the influence of shape and agglomeration on the silicate profiles are lagging behind theoretical computations of this effect. Such studies may open a way to discriminate between the origin of crystalline silicates from annealing or direct condensation from the gas phase. The latter process is poorly understood and is presently lacking a firm experimental basis. We can expect to see a flood of new observational data coming from Spitzer, especially for sources which are too faint to have been observed with ISO. In addition, Herschel and SOFIA will soon provide more information on the far-infrared properties of cosmic silicates.

Acknowledgements

We would like to thank our collaborators J. Bouwman, J. Dorschner, C. Koike, R. van Boekel, and L.B.F.M. Waters for many interesting discussions and for providing material for this review.

References

- Agladze, N.I., Sievers, A.J., Jones, S.A., Burlitch, J.M., & Beckwith, S.V.W. 1996, *Ap. J.* 462, 1026
- Apai, D., Pascucci, I., Bouwman, J., Natta, A., Henning, Th., & Dullemond, C.P. 2005, *Science* 310, 834.
- Beichman, C.A., Bryden, G., Gautier, T.N., Stapelfeldt, K.R., Werner, M.W., Misselt, K., Rieke, G., Stansberry, J., & Trilling, D. 2005, *Ap. J.* 626, 1061
- Boudet, N., Mutschke, H., Nayral, C., Jäger, C., Bernard, J.-P., Henning, Th., & Meny, C. 2005, *Ap. J.* 633, 272
- Bouwman, J., Meeus, G., de Koter, A., Hony, S., Dominik, C., & Waters, L.B.F.M. 2001, *A&A* 375, 950
- Bouwman, J., *et al.*, 2005, in preparation
- Bowey, J.E., Lee, C., Tucker, C., Hofmeister, A.M., Ade, P.A.R., & Barlow, M.J. 2001, *MNRAS* 325, 886
- Bowey, J.E., Barlow, M.J., Molster, F.J., Hofmeister, A.M., Lee, C., Tucker, C., Lim, T., Ade, P.A.R., & Waters, L.B.F.M. 2002, *MNRAS* 331, L1
- Bradley, J. 1994, *Science* 265, 925
- Cameron, M. & Papike, J.J. 1980 in *Reviews in Mineralogy Vol. 7; Pyroxenes*, ed. Ch.T. Prewitt (BookCrafters, Inc.: Chelsea), p. 5
- Colangeli, L., Henning, Th., Brucato, J.R., Henning, Th., Brucato, J.R., Clément, D., Fabian, D., Guillois, O., Huisken, F., Jäger, C., Jessberger, E.K., Jones, A., Ledoux, G., Manicò, G., Mennella, V., Molster, F.J., Mutschke, H., Pirronello, V., Reynaud, C., Roser, J., Vidali, G., & Waters, L.B.F.M. 2003, *Astron. Ap. Rev.* 11, 97
- Crovisier, J., Leech, K., Bockelée-Morvan, Brooke, T.Y., Hanner, M.S., Altieri, B., Keller, H.U., & Lellouch, E. 1997, *Science* 275, 1904
- Chiang, E.I. & Goldreich, P. 1997, *Ap. J.* 490, 368
- Chihara, H., Koike, C., & Tsuchiyama, A. 2001, *Publ. Astron. Soc. Japan* 53, 243
- Chihara, H., Koike, C., Tsuchiyama, A., Tachibana, S., & Sakamoto, D. 2002, *A&A* 391, 267
- Demyk, K., Carrez, P., Leroux, H., *et al.* 2001, *A&A* 368, L38
- Dorschner, J., Begemann, B., Henning, Th., Jäger, C., & Mutschke, H. 1995, *A&A* 300, 503
- Dupac, X., Bernard, J.-P., Boudet, N., Giard, M., Lamarre, J.-M., M'eny, C., Pajot, F., Ristorcelli, I., Serra, G., Stepnik, B., & Torre, J.-P. 2003, *A&A* 404, L11
- Dukes, C., Baragiola, R., & McFadden, L. 1999, *Geophys. Res.* 104, 1865
- Fabian, D., Jäger, C., Henning, Th., Dorschner, J., & Mutschke, H. 2000, *A&A* 364, 282
- Fabian, D., Henning, Th., Jäger, C., Mutschke, H., Dorschner, J., & Wehrhan, O. 2001, *A&A* 378, 228
- Forrest, W.J., Sargent, B., Furlan, E., D'Alessio, P., Calvet, N., Hartmann, L., Uchida, K.I., Green, J.D., Watson, D.M., Chen, C.H., Kemper, F., Keller, L.D., Sloan, G.C., Herter, T.L., Brandl, B.R., Houck, J.R., Barry, D.J., Hall, P., Morris, P.W., Najita, J., & Myers, P.C. 2004, *Ap. J. Suppl.* 154, 443
- Gail, H.-P. 2004, *A&A* 413, 571
- Gervais, F., Blin, A., Massiot, D., Coutures, J.P., Chopinet, M.H., & Naudin, F. 1987, *J. Non-Cryst. Sol.* 89, 384
- Hallenbeck, S.L., Nuth, J.A., & Daukantas, P.L. 1998, *Icarus* 131, 198
- Hao, L., Spoon, H.W.W., Sloan, G.C., Marshall, J.A., Armus, L., Tielens, A.G.G.M., Sargent, B., van Bemmelen, I.M., Charmandaris, D.W., Weedman, D.W., & Houck, J.R. 2005, *Ap. J.* 625, L75
- Henning, Th. 2003a, in *Solid State Astrochemistry*, eds. V. Pirronello, Krelowski, J. & G. Manicò (Kluwer: Dordrecht), p. 85

- Henning, Th., ed. 2003b, *Astromineralogy* (Springer:Berlin)
- Henning, Th. & Stognienko, R. 1996, *A&A* 311, 191
- Henning, Th. & Mutschke, H. 1997, *A&A* 327, 743
- Henning, Th., Il'in, V.B., Krivova, N.A., Michel, B., & Voshchinnikov, N.V. 1999, *A&AS* 136, 405
- Hofmeister, A.M. 1997, *Phys. Chem. Minerals* 24, 535
- Jäger, C., Molster, F.J., Dorschner, J., Henning, Th., Mutschke, H., & Waters, L.B.F.M. 1998, *A&A* 339, 904
- Jäger, C., Dorschner, J., Mutschke, H., Posch, Th., & Henning, Th. 2003a, *A&A* 408, 193
- Jäger, C., Il'in, V.B., Henning, Th., Mutschke, H., Fabian, D., Semenov, D.A., & Voshchinnikov, N.V. 2003b, *J. Quant. Spectr. Rad. Transfer* 79-80, 765
- Jäger, D. Fabian, C., Schrepel, F., Dorschner, J., Henning, Th., & Wesch, W. 2003c, *A&A* 401, 57
- Kessler-Silacci, J.E., Hillenbrand, L.A., Blake, G.A., & Meyer, M.R. 2005, *Ap. J.* 622, 404
- Koike, C., Chihara, H., Tsuchiyama, A., Suto, H., Sogawa, H., & Okuda, H. 2003, *A&A* 399, 1101
- Koike, C., Mutschke, H., Suto, H., Naoi, T., Chihara, H., Henning, Th., Jäger, C., Tsuchiyama, A., Dorschner, J., & Okuda, H. 2005, *A&A*, in press
- Malfait, K., Waelkens, C., Waters, L.B.F.M., Vandebussche, B., Huygen, E., & de Graauw, M.S. 1998, *A&A* 332, 25
- Menshchikov, A.B. & Henning, Th. 1997, *A&A* 318, 879
- Meeus, G., Waters, L.B.F.M., Bouwman, J., van den Ancker, M.E., Waelkens, C., & Malfait, K. 2001, *A&A* 365, 476
- Mennella, V., Brucato, J.R., Colangeli, L., Palumbo, P., Rotundi, A., & Bussoletti, E. 1998, *Ap. J.* 496, 1058
- Messenger, S., Keller, L.P., Stadermann, F.J., Walker, R.M., & Zinner, E. 2003, *Science* 300, 105
- Min, M., Hovenier, J.W., & de Koter, A. 2005, *A&A* 432, 909
- Molster, F.J., Waters, L.B.F.M., Tielens, A.G.G.M., Koike, C., & Chihara, H. 2002, *A&A* 382, 441
- Mostefaoui, S. & Hoppe, P. 2004, *Ap. J.* 613, L149
- Mutschke, H., Begemann, B., Dorschner, J., Gürtler, J., Gustafson, B., Henning, Th., & Stognienko, R. 1998, *A&A* 333, 188
- Mysen, B.O., Virgo, D., & Seifert, F.A. 1982, *Rev. Geophys. Space Phys.* 20, 353
- Natta, A., Meyer, M.R., & Beckwith, S.V.W. 2000, *Ap. J.* 534, 838
- Nguyen, A.N. & Zinner, E. 2004, *Science* 303, 1496
- Przygodda, F., van Boekel, R., Àbràham, P., Melnikov, S.Y., Waters, L.B.F.M., & Leinert, C. 2003, *A&A* 412, L43
- Servoin, J.L. & Piriou, B. 1973, *Phys. Stat. Sol. (b)* 55, 677
- Scott, A. & Duley, W.W. 1996, *Ap. J. Suppl.* 105, 401
- Scott, E.R. & Krot, A.N. 2005, *Ap. J.* 623, 571
- Siebenmorgen, R., Haas, M., Krügel, E., & Schulz, B. 2005, *A&A* 436, L5
- Sturm, E., Schweitzer, M., Lutz, D., Contursi, A., Genzel, *et al.* 2005, *Ap. J.* 629, L21
- Suto, H., Koike, C., Sogawa, H., Tsuchiyama, A., Chihara, H., & Mizutani, K. 2002, *A&A* 389, 568
- Tamanai, A., *et al.*, 2005, in preparation
- van den Ancker, M.E., Bouwman, J., & Wesselius, P.R. 2000, *A&A* 357, 325
- van Boekel, R., Waters, L.B.F.M., Dominik, C., Bouwman, J., de Koter, A., Dullemond, C.P., & Paresce, F. 2003, *A&A* 400, L21.
- van Boekel, R., Min, M., Leinert, Ch., Waters, L.B.F.M., Richichi, *et al.* 2004, *Nature* 432, 479
- van Boekel, R., Min, M., Waters, L.B.F.M., de Koter, A., Dominik, C., van den Ancker, M.E., & Bouwman, J. 2005, *A&A*, 437, 189
- Voshchinnikov, N.V., Il'in, V.B., & Henning, Th. 2005, *A&A* 429, 371
- Yada, T., Stadermann, F.J., Floss, C., Zinner, E., Olinger, C.T., Graham, G.A., Bradley, J.P., Dai, Z.R., Nakamura, T., Noguchi, T., & Bernas, M. 2005 *Lunar Planet. Sci.* 36, 1227